

See discussions, stats, and author profiles for this publication at: <https://www.researchgate.net/publication/268821527>

# Paleo-environment and flooding of the Limpopo River-plain, Mozambique, between c. AD 1200–2000

Article in *Catena* · November 2014

DOI: 10.1016/j.catena.2014.10.038

---

CITATIONS

5

READS

228

7 authors, including:



[Jan Risberg](#)

Stockholm University

59 PUBLICATIONS 757 CITATIONS

[SEE PROFILE](#)



[Ian Frederick Snowball](#)

Uppsala University

148 PUBLICATIONS 3,352 CITATIONS

[SEE PROFILE](#)



[Karin Holmgren](#)

Swedish University of Agricultural Sciences

85 PUBLICATIONS 5,471 CITATIONS

[SEE PROFILE](#)



[João Mugabe](#)

Eduardo Mondlane University

7 PUBLICATIONS 38 CITATIONS

[SEE PROFILE](#)

Some of the authors of this publication are also working on these related projects:



Exploring precolonial agriculture and intensification: the case of Bokoni, South Africa [View project](#)



Disco Climate (2009-2012) [View project](#)

All content following this page was uploaded by [Elin Norström](#) on 24 March 2015.

The user has requested enhancement of the downloaded file. All in-text references [underlined in blue](#) are added to the original document and are linked to publications on ResearchGate, letting you access and read them immediately.



## Paleo-environment and flooding of the Limpopo River-plain, Mozambique, between c. AD 1200–2000

Sandra Raúl Sítroe <sup>a,b,c,\*</sup>, Jan Risberg <sup>b,c</sup>, Elin Norström <sup>b,d</sup>, Ian Snowball <sup>e,f</sup>, Karin Holmgren <sup>b,c</sup>,  
Mussa Achimo <sup>a</sup>, João Mugabe <sup>a</sup>

<sup>a</sup> Department of Geology, University of Eduardo Mondlane, Maputo, Mozambique

<sup>b</sup> Bert Bolin Centre for Climate Research, Stockholm University, S-106 91 Stockholm, Sweden

<sup>c</sup> Department of Physical Geography and Quaternary Geology, Stockholm University, S-106 91 Stockholm, Sweden

<sup>d</sup> Department of Geological Sciences, Stockholm University, S-106 91 Stockholm, Sweden

<sup>e</sup> Department of Geology-Quaternary Sciences, Lund University, Sölvegatan 12, S-223 62 Lund, Sweden

<sup>f</sup> Department of Earth Sciences-Natural Resources and Sustainable Development, Uppsala University, Villavägen 16, S-752 36 Uppsala, Sweden



### ARTICLE INFO

#### Article history:

Received 24 March 2014

Received in revised form 28 October 2014

Accepted 31 October 2014

Available online xxxx

#### Keywords:

Flooding events

Mineral magnetism

Limpopo River

Diatoms

Mozambique

### ABSTRACT

Multi-proxy analysis was performed on a radiocarbon-dated core, collected from a relic oxbow lake in the Limpopo River-plain, Mozambique, with the aim to reconstruct paleo-environment and past flooding of the lower river system over the past c. 800 years. An additional objective was to evaluate and investigate the potential use of different proxies as recorders of paleo-flooding events and paleo-environmental variability within the floodplain. The proxies applied in this study were: mineral magnetic properties, grain-size distribution, organic carbon content and diatom microfossil assemblages. We found that sediment grain-size and mineral magnetic properties of the minerogenic fraction were the most sensitive proxies in terms of detecting signals from high-intensity river-discharge events. In the 800 year long sequence, variations in sand content, magnetic susceptibility and saturation isothermal remnant magnetization suggest at least four major flooding events at the site during the reconstructed period; in the mid-1200, late-1300, mid-1500 AD and during the last century. The diatom proxy reflects the development of the site from an open oxbow lake to a mainly terrestrial area. The diatom assemblage indicates that open lake conditions prevailed at the site between c. AD 1200–1400, with periodic inundation by marine water, most likely due to late Holocene sea-level changes. From c. AD 1400 and onwards, diatoms were rarely deposited at the site, which indicates drier conditions. This was a result of soil formation and gradual in-filling of the lake, a process which possibly was accentuated by a regionally dry climate situation. Our study shows that oxbow lakes and the proxies used here have great potential for reconstructing flooding events, a knowledge that is crucial for potential prediction and mitigation of flooding events in Mozambique in the future. Although chronological uncertainties limit comparisons to other paleo-environmental records, it seems that the flooding events recorded at our site occurred both during regionally wet and dry periods. Our data infer however, that flooding was probably more clearly recorded during the lake-stages than during infilled stage, probably as the terrestrial environment was more exposed to erosion.

© 2014 Elsevier B.V. All rights reserved.

### 1. Introduction

Understanding of past climate dynamics and hydrological conditions is necessary for the evaluation of climate model predictions, as well as for quantifying corresponding climate changes and uncertainties during the present and in the future (Hegerl and Russel, 2011). General Circulation Model (GCM) predictions of future climate change remain complex

and uncertain, particularly regarding humidity patterns in sub-tropical and tropical regions of Africa, where precipitation scenarios project different trend and magnitude of future change (IPCC, 2013). Therefore, there is uncertainty regarding future rainfall variability in southern Africa, both regarding its spatial and frequency distributions and the occurrence of extreme rainfall events. Rainfall events cause flooding events in southern Africa and are considered to be a serious natural hazard (Stal, 2011). A modern example of this hazard was the flooding associated with the tropical cyclone Eline, which affected parts of Mozambique, South Africa and Zimbabwe in AD 2000 (Reason and Keibell, 2004). Cardoso (2009) estimated that the peak discharge caused by the Eline cyclone has a 50-year return period. In general, severe flooding events in the region have a return period of 10–25 years, while the normal or moderate

\* Corresponding author at: Department of Geology, Av. Moçambique, Km 1.2, CP. 257, Maputo, Moçambique. Bert Bolin Centre for Climate Research and Department of Physical Geography and Quaternary Geology, Stockholm University, S-106 91 Stockholm, Sweden. Tel.: +258 21 475280, +46 72 9149664; fax: +258 21 475280.

E-mail addresses: [sandrasitoe@yahoo.com.br](mailto:sandrasitoe@yahoo.com.br), [sandra.sitoe@natgeo.su.se](mailto:sandra.sitoe@natgeo.su.se) (S.R. Sítroe).

flooding events have a return period of 2–5 years (Cardoso, 2009). The loss of several hundred lives and damage to infrastructure, in the wake of the Eline cyclone, had serious negative effects on social and economic development of southern Mozambique. The Eline cyclone and its aftermaths, stress the importance to predict rainfall variability and the past recurrence interval of river flooding. Improved understanding of rainfall variability and flood frequencies would help society to take appropriate mitigatory actions and prepare for similar events in the future.

An increasing number of records of hydro-climate and flooding events in southern Africa are available, based on instrumental data (e.g. Dyson and Von Heeren, 2001; Mélice and Reason, 2007) and pre-instrumental reconstructions (e.g. Smith, 1991; Hattingh and Zawada, 1996; Smith and Zawada, 1990; Ekblom and Stabell, 2008; Heine and Heine, 2002; Holmgren et al., 2012). Historically documented flooding events generally coincide with those recorded in slack water sediments. However, most studies are based on discontinuous records and the dating of events is often uncertain. Moreover, most current research focuses on the causes of instrumentally recorded flood events, i.e. those that took place during the last century (e.g. Reason, 2007; Reason and Keibel, 2004). Considerably less is known about long-term frequency of flood events, as well as the magnitude of paleo-flooding events and the paleo-environment of the affected flood-plain. One reason for this knowledge gap is probably the many challenges associated with the use of river sediments as a source of paleodata in this region. For example, the preservation of micro- and macrofossils is hampered by temporary droughts (pollen, spores, seeds are oxidized) and high pH (diatoms, phytoliths are degraded). Furthermore, frequent shifts in river level may result in uneven deposition of sediments, sometimes

with unknown origin, and erosive processes associated with the river flow may affect the continuity of the record, causing sediment hiatuses. Additionally, radiocarbon dating is complex due to possible reworking of macrofossils and hard water effects. Thus, there is an urgent need to evaluate different proxies that reflect flooding intensity and frequency in this area.

With this study, we address the lack of paleo-flood proxies in southern Mozambique, and make a first attempt to reconstruct past flooding events and hydrological conditions in the Limpopo River flood-plain, through a multi-proxy analysis of a sediment core retrieved from a relic oxbow lake located within the flood-plain (Fig. 1). The retrieved sediment core covers the last c. 800 years. An additional objective is to evaluate the different proxy methods used, and specify suitable approaches to detecting paleo-floods in river sediments in this area. More specifically, we investigate the potential of mineral magnetic properties, grain size distribution, carbon content and diatom microfossil assemblages as recorders of paleo-flooding events and paleoenvironmental variability within the floodplain. Furthermore, we discuss problems involved in radiocarbon dating of river sediments in this region, and identify the most suitable approach to dating sediments that accumulated within the Limpopo River flood-plain.

### 1.1. Study site

The Limpopo River and its catchment are located in the south-eastern part of Africa, and cover approximately 412,000 km<sup>2</sup> (Fig. 1). The catchment has a population of 13.5 million habitants, which is distributed within parts of Botswana, Mozambique, South Africa and Zimbabwe.

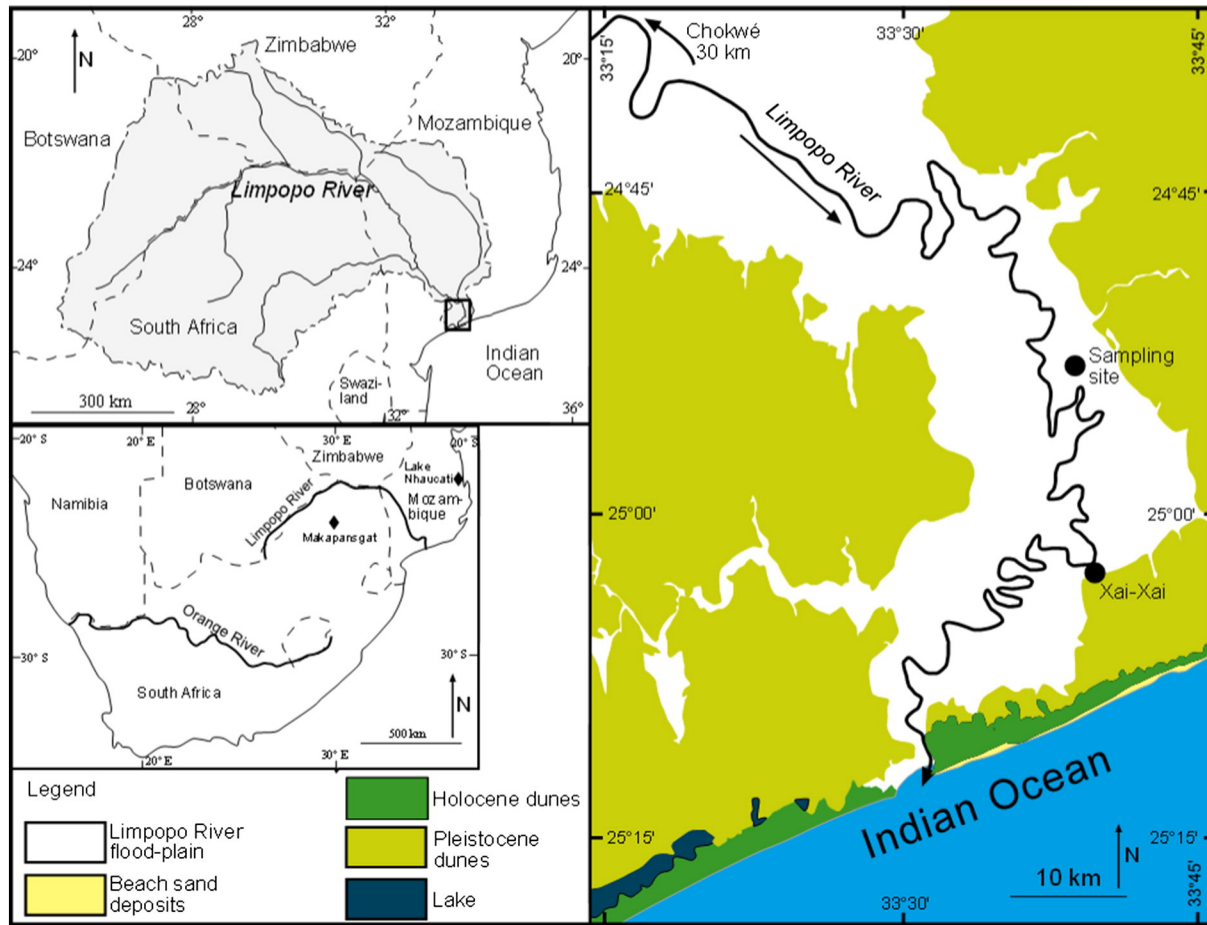


**Fig. 1.** Upper left: Map showing Limpopo River drainage area and the riparian countries. The study area is marked with a square. Right: map showing parts of the flood plain located within Mozambique, including the sampling site and the provincial capital Xai-Xai. Lower left: Map over southern Africa and some of the sites mentioned in the text. Adapted from INGC et al. (2003) and GTK Consortium (2006).

The lower course of the river flows through southern Mozambique with a flood-plain covering about 79,600 km<sup>2</sup>. The flood-plain is a flat area that extends approximately 200 km in the NE–SW direction and 50 km in the NE–SW direction (INGC et al., 2003). Relic oxbow lakes that have been filled with sediment are abundant as a consequence of the meandering river, with present day oxbow lakes in different stages of development. The relic oxbow lakes are seen as shallow topographical features (depressions) basins in an undulating landscape. The natural hydrology has been modified by the constructions of dams upstream since the 1940s, which probably altered the meandering activity. The river is flanked by pronounced levees that reach about 1–2 m above the flood-plain. The flood-plain is fertile and used for both cultivation and grazing. At the river mouth, extensive Pleistocene dune formations impound river water on its way to the ocean (Fig. 1). The narrow opening to the ocean, the altitude of the dunes (about 35 m a.s.l.) and the gentle slope make the flood-plain and its habitants susceptible to the impacts of high intensity rainfall events.

The sampling site is a relic oxbow lake (24°53'28.5"S, 33°38'28.4"E) that is presently used primarily for grazing, but it can be inundated by water during flooding events. It is located approximately 60 km from the river mouth (Fig. 1), at an altitude of 6 m a.s.l. The relic oxbow lake is approximately 3 km long and 200 m wide. The area is almost flat but has a gently undulating surface as a result of the lateral accretion of sediments from the meandering system of the Limpopo River. A minor topographic depression at the site suggests that re-connection to the main Limpopo River may occur during high water stands. The topography at the sampling site results in an environment where inundating floods will first erode and transport sediment downstream. During the recession of the flood, suspended sediment in the trapped flood water will be deposited on the bed of the basin.

Eleven flooding events occurred in the Limpopo River flood-plain area (including the sampling site) during the last century; AD 1915, 1937, 1955, 1967, 1972, 1975, 1977, 1981, 2000, 2012 and 2013. The first two are documented in newspapers printed in 1967, while the next six events are registered in reports from Direcção Nacional de Águas (1996) and the last three events are from recent observations. The magnitude of flooding depends mainly on amount and intensity of rainfall, in combination with the size and location of the geographical area being affected by the rain storm. Furthermore, the dam constructions upstream the Limpopo River have altered the natural hydrographic regime and can mitigate "natural" flooding events in the flood-plain. However, during events when the level of water trapped behind the dams becomes a threat to the infrastructure water will be released and potentially cause flash floods to occur in the flood-plain. Generally, the runoff is high in the upper part of the floodplain, near Chokwé, and decreases where the floodplain becomes shallower and wider. During the most recent flooding events in 2013, the majority of rainfall was received upstream of the flood-plain area, and the water level was higher near our sampling site than in the downstream Xai-Xai area. This pattern was also observed during the January 2013 flooding event, when the water source (intense rainfall) was located further upstream from the floodplain area. This resulted in high water fluxes and flooding of a large part of the Chokwé City, while, Xai-Xai City, located further downstream, was not affected. Interruptions of road connections during this flooding event made it impossible to access the sampling site and we could therefore not assess whether that area was flooded or not.

## 2. Materials and methods

### 2.1. Sampling

During fieldwork in 2007, a 4.68 m long sediment core was collected using a 1.2 m long gouge auger with an inner diameter of 60 mm, and a piston corer, 75 cm long with an inner diameter of 50 mm (both corers were manufactured by Eijkelkamp). The gouge auger was used to

sample the upper 2 m and the piston corer was used for the remaining part of the sequence. The sediment sequence was sub-sampled at 1 cm contiguous intervals.

### 2.2. Radiocarbon dating and calibration

Ten samples were submitted for radiocarbon dating (Table 1). Dating was performed on shells (three samples), wood macrofossil (one sample) and bulk sediment (six samples), at the Ångström Laboratory, Uppsala, Sweden, and at the Poznan Radiocarbon Laboratory, Poland. Two living shells from the flood-plain were also dated for comparison. The <sup>14</sup>C-ages were calibrated using the OxCal calibration program version 4.0 and the Southern Hemisphere calibration curve ShCal04 (McCormac et al., 2004). Calibrated ages are expressed in years AD.

### 2.3. Grain size, organic carbon and water content

Samples from every second centimeter were sieved through a 63 µm mesh to determine the sand content. Approximately 4 g of sediment was dispersed in 100 ml of 0.05% Calgon® (Na<sub>4</sub>PO<sub>4</sub>). The samples were wet-sieved after a night in a shaking table. The sand fraction (>63 µm) was dried overnight in an oven at 60 °C, and weighed to calculate the proportion of the total sample. The lower part of the core also include some occasional gravel, which are included in the >63 µm sand fraction. The clay and silt content was determined using a SediGraph 5100. Organic carbon content was measured every second centimeter, on the same sample levels as the grain size analysis, in an ELTRA CS 500 carbon sulphur determinator. The samples were ground and oven dried at 60 °C for 1 h. A total of 150–200 mg per sample was run in the carbon determinator at 550 °C. The method is based on combustion, oxidation of carbon to CO<sub>2</sub> and analyses of the gas through infrared absorption. The water content was calculated through weighing samples before and after drying them.

### 2.4. Diatoms

Diatom microfossils were extracted from 37 samples using approximately 2 g of dry sediment (Battarbee, 1986). Samples were acidified with 10% HCl to remove carbonates and 17% H<sub>2</sub>O<sub>2</sub> to oxidize organic matter. Once all the organic matter was removed, distilled water was added to the residue in 100 ml beakers. Clay was removed by repeated decanting at 2 h intervals. 5% NH<sub>3</sub> was used to disperse clay particles. The remaining material was spread onto a cover glass and mounted in Naphrax®. Diatom analysis was carried out under a ZEISS Axiophot Microscope using 1000× magnification. The diatoms were present in low numbers, which made it difficult to count the 300 frustules recommended for statistical treatment (Battarbee, 1986). In general about 100 diatoms were counted per sample, lower counts were generally restricted to the upper part of the section due to low concentration or sometimes the complete absence of diatoms. Species identification and their ecological preferences were based on Cholnoky (1957), Giffen (1963, 1966a, 1966b, 1970, 1971, 1973, 1975, 1976), Foged (1975), Gasse (1986), Krammer and Lange-Bertalot (1986, 1988, 1991a,b), Risberg (1988), Round et al. (1990), Vos and De Wolf (1993), Round and Basson (1997) and Witkowski et al. (2000).

### 2.5. Mineral magnetic parameters

The mineral magnetic parameters were measured on all the 1 cm contiguous sub-samples in the Palaeomagnetic Laboratory in the Department of Geology-Quaternary Sciences, Lund University, Sweden following standard procedures that are described by, for example, Thompson and Oldfield (1986). Magnetic susceptibility ( $\chi$ ) was measured on a Geofyzica Brno KLY-2 Kappabridge. Anhysteretic Remanent Magnetization (ARM) was induced using 2G-Enterprises

**Table 1**

Results of the radiocarbon dating of material from the oxbow lake sediments. The depth of dated sample is indicated with reference to the present ground surface. Two living shells from the flood plain were dated in addition to the fossil material, showing modern age and therefore with  $^{14}\text{C}$ -ages expressed in percent modern carbon (pMC).

Depth (cm)	Lab code	$^{14}\text{C}$ years BP	Calibrated age AD ( $1\sigma$ )	Calibrated age AD ( $2\sigma$ )	Dated material
40–50	Poz-25218	510 ± 30	1420–1450 (68.2%)	1405–1460 (95.4%)	Bulk
103–113	Poz-25219	890 ± 30	1160–1225 (68.2%)	1050–1060 (1%)	Bulk
				1150–1270 (94.4%)	
143–153	Poz-25220	1480 ± 30	605–655 (68.2%)	570–665 (95.4%)	Bulk
190–191	Ua-35111	355 ± 30	1505–1590 (59.3%)	1485–1645 (95.4%)	Shell
			1615–1630 (8.9%)		
233–238	Poz-26170	1460 ± 30	580–640 (68.2%)	550–650 (95.4%)	Bulk
233–239	Ua-34665	350 ± 40	1500–1590 (56.2%)	1475–1650 (95.4%)	Shell (bivalve)
			1615–1635 (12.0%)		
303–304	Ua-34566	620 ± 40	1320–1350 (36.8%)	1300–1430 (95.4%)	Shells (gastropoda)
			1385–1410 (31.4%)		
348–353	Poz-25221	1340 ± 30	675–725 (40.7%)	655–780 (93.7%)	Bulk
			740–770 (27.5%)	790–805 (1.7%)	
383–388	Poz-25222	1610 ± 30	430–495 (41.9%)	420–580 (95.4%)	Bulk
			505–550 (26.3%)		
448–449	Ua-35112	880 ± 35	1175–1230 (60.7%)	1050–1060 (0.8%)	Wood fragment
			1250–1265 (7.5%)	1150–1275 (94.6%)	
Floodplain/surface	Poz-51547	105.72 ± 0.32 pMC	1998 or 1959 AD	–	Living shell (gastropoda)
Floodplain/surface	Ua-45401	103.3 ± 0.3 pMC	1998 or 1958 AD	–	Living shell (gastropoda)

demagnetization coils in a peak AF of 100 milliTesla (mT) and a direct bias field of 0.1 mT. Saturation Isothermal Remanent Magnetization (SIRM) was induced in a Redcliffe 700 BSM pulse magnetizer at 1 T. Backfields were induced with the pulse magnetizer at –100 and –300 mT to determine S-ratios, where  $S_{100} = S_{-100}/\text{SIRM}$  and  $S_{300} = S_{-300}/\text{SIRM}$ . The high field isothermal remanence (HIRM) was also calculated. The isothermal remanent magnetizations (IRM) were measured with a Molspin Minispin and the ARM was divided by the bias field to calculate the susceptibility of ARM ( $\chi_{\text{ARM}}$ ). Mass specific values were calculated on the basis of dry mass and are presented in SI units.

### 3. Results

#### 3.1. Chronology

The resulting age–depth model is illustrated in Fig. 2, with calibrated ages plotted with their  $2\sigma$  uncertainty range. The model was based on linear interpolation between the highest probability points, with the exception of Ua-35111, where the second highest probability point was considered more realistic, as accumulation rates would otherwise be inferred to be negative. The dates from the living shells did not suggest a problem of reservoir age as they were dated as modern (Table 1). The

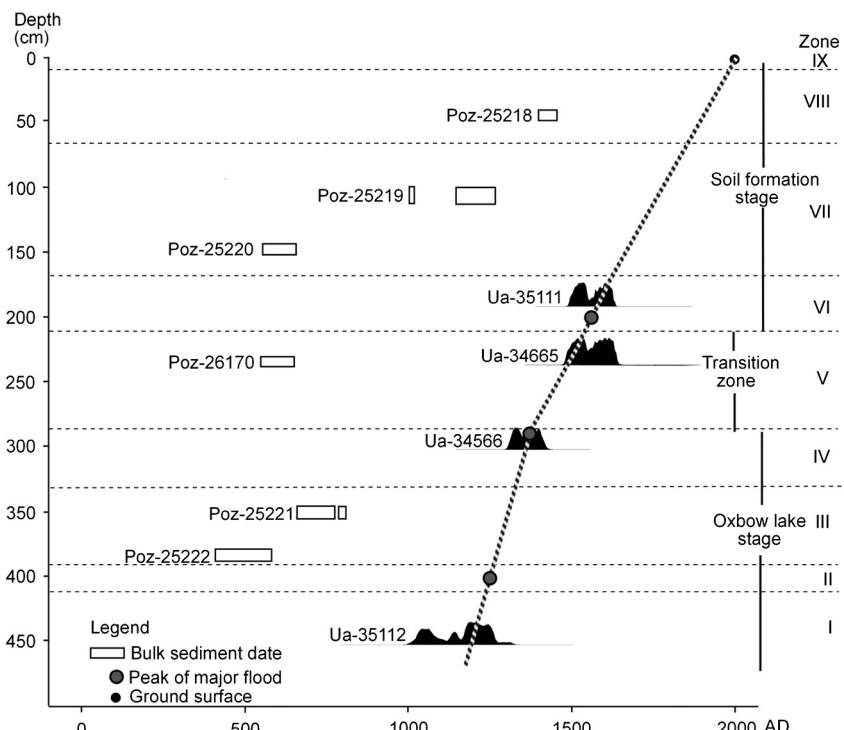


**Fig. 2.** Lithology, sand content, organic carbon content and water content profiles for the complete sequence. Zones I–IX are the result of the combined interpretation of  $\chi$ , ARM, SIRM and  $\chi_{\text{ARM}}/\text{SIRM}$ .

bulk samples have older ages than the macrofossils found at similar depths, a problem which is discussed further below.

### 3.2. Lithology, grain size, organic carbon and water content

The lithology is characterized by shifts between clay, silty clay and silty sand (Fig. 3). All boundaries between lithological units were gradational and no abrupt transitions were visually observed. The sediment colors range from gray in the bottom to dark brown at the top. Occasional gastropods, bivalves and wood macrofossils were found in the lower part (448–113 cm) and these were used for  $^{14}\text{C}$ -dating. Modern roots were present in the uppermost section (0–40 cm). The organic carbon content (Fig. 3) is generally low throughout the core, only varying within a span from about 0 to 1%, with the highest carbon values displayed in the lower section. Water content varies between approximately 5% and 30%, with slightly higher values in the lowermost section. The grain size parameter, i.e. the sand content, fluctuates between 1% up to nearly 30%, showing four distinct peaks, centered at depths of 81, 200, 290 and 405 cm.

### 3.3. Diatoms

The diatom analysis resulted in identification of a total 60 diatom taxa, of which the most abundant ones are illustrated (Fig. 4a) and grouped according to salinity preferences (Fig. 4b). Three diatom zones were identified.

#### 3.3.1. Diatom zone 1 (468–280 cm, c. AD 1200–1400)

This zone contains a moderate number of diatoms and the flora is characterized by a mixture of freshwater taxa (e.g. *Aulacoseira granulata*), halophilous taxa (*Cyclotella meneghiniana*), brackish-marine taxa (e.g. *Nitzschia compressa*, *Diploneis interrupta*, *Terpsinoë americana*, *Actinopytchus* spp., *Coscinodiscus* sp., *Nitzschia cocconeiformis*) and aerophilous taxa (*Hantzschia amphioxys*, *Navicula goeppertiana*, *Pinnularia borealis*).

#### 3.3.2. Diatom zone 2 (280–215 cm; c. AD 1400–1700)

This sequence is characterized by a decrease in diatom abundance and the only diatom species present is the halophilous taxa, *C. meneghiniana*.

#### 3.3.3. Diatom zone 3 (215–0 cm; AD 1700–2000)

Zone 3 is represented by the presence of brackish-marine taxa (*D. interrupta*, *Stauroneis legumen*), indifferent taxa (*Amphora libya*, *Fragilaria brevistrata*, *Neidium iridis*), freshwater taxa (*Aulacoseira ambigua*, *Cymbella silesiaca*, *Gomphonema augustum*, *Gomphonema* sp., *Pinnularia biceps*) and aerophilous taxa (*Hantzschia amphioxys*, *N. goeppertiana*). The diatom concentration is low, as in the underlying zone 2.

### 3.4. Mineral magnetic parameters

The results from the analysis of mineral magnetic parameters ( $\chi$ , ARM, SIRM, S-ratio, HIRM, medium IRM, and the calculated ratios  $\chi_{\text{ARM}}/\text{SIRM}$ ,  $\text{SIRM}/\chi$ ) are illustrated in Fig. 5. Based on the variations in magnetic susceptibility, ARM, SIRM and grain size, nine stratigraphic zones were identified (Table 2, Fig. 5).

## 4. Interpretation

### 4.1. Chronology

The radiocarbon dating and age-depth construction reveal a significant offset between bulk sample ages and macrofossil ages (Fig. 2). The age difference between these sample categories at corresponding depths ranges between c. 500 and 1000 years. The relatively older age of the bulk sediment samples probably results from that secondary organic matter has been reworked from upstream and/or the effect of tertiary limestone that has been eroded and transported from old soil sequences, also from upstream areas.

The dates based on shells and the wood fragment follows a coherent stratigraphic-chronological order and can be combined to construct a reasonable age model (Fig. 2). The living shells collected on the ground

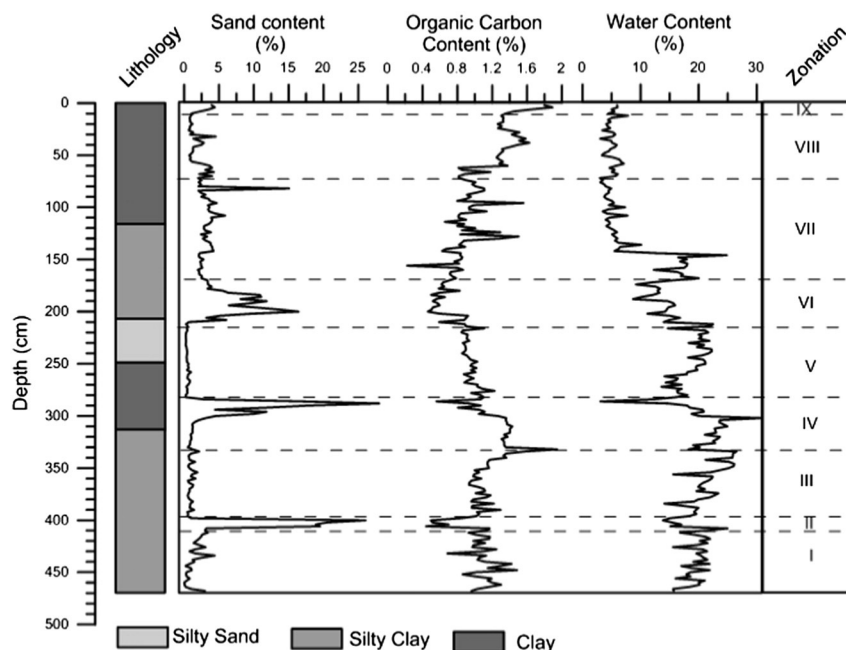


**Fig. 3.** Age-depth model for the sampling site in the Limpopo River flood-plain. Bulk sediment dates indicate reservoir ages of 500–1000 years (white boxes). We considered the dates of macrofossils (black graphs showing their probability distributions) as most reliable for age-model construction, see discussion in text. The zones I–IX were defined based on the variations mainly in  $\chi$ , SIRM and grain-size.

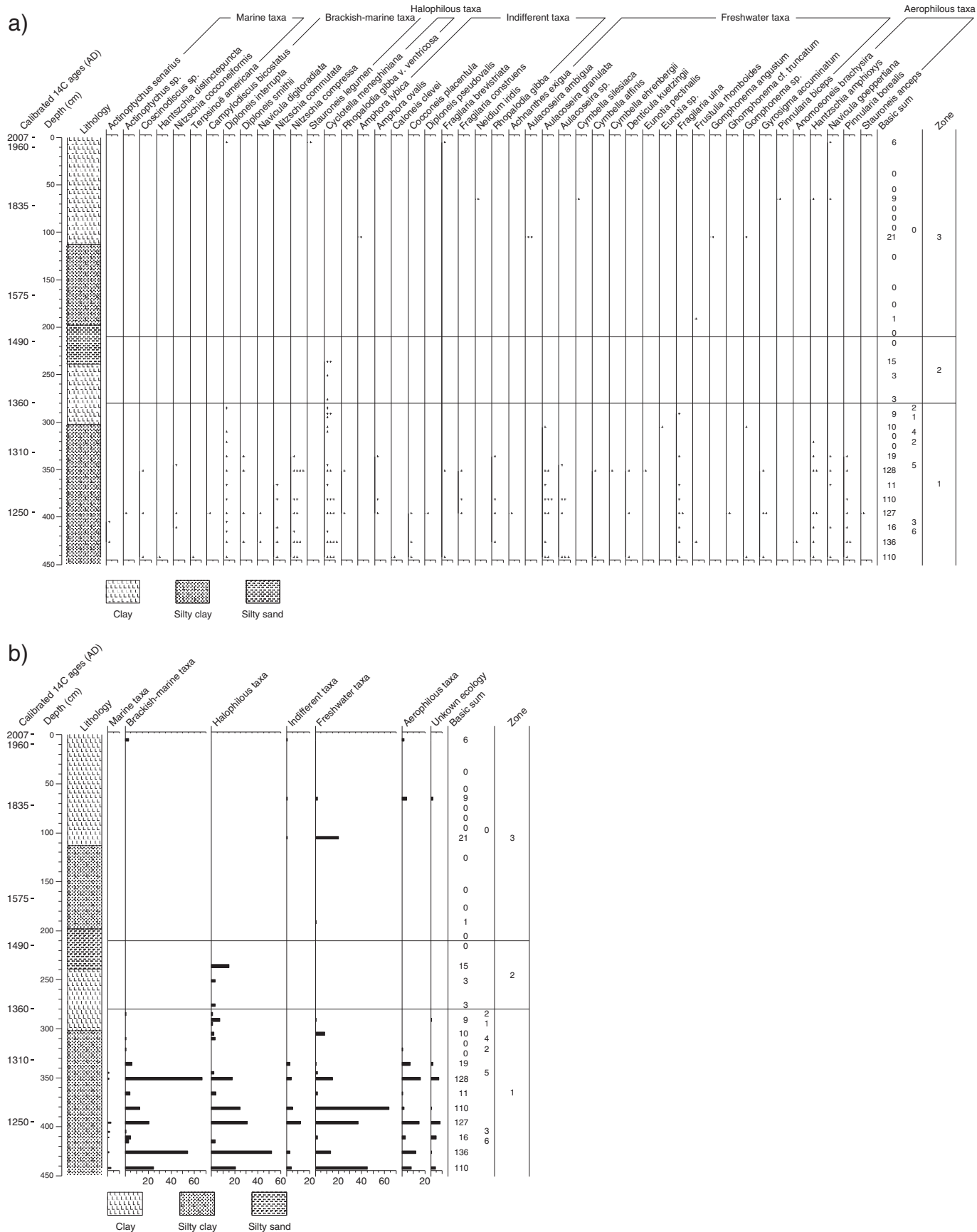


**Fig. 4.** a) Relative distribution of the most abundant diatoms, excluding species with unknown ecology. Since basic sums in all depths counted are lower than 300 frustules recommended for statistical treatment (Battarbee, 1986), we have chosen to present their abundance on a relative scale based on the following system: (+): 1–5 frustules/sample, (++) 6–20 frustules/sample, (+++) 21–50 frustules/sample, (++++) >51 frustules/sample. b) The diatom taxa grouping according to salinity preferences.

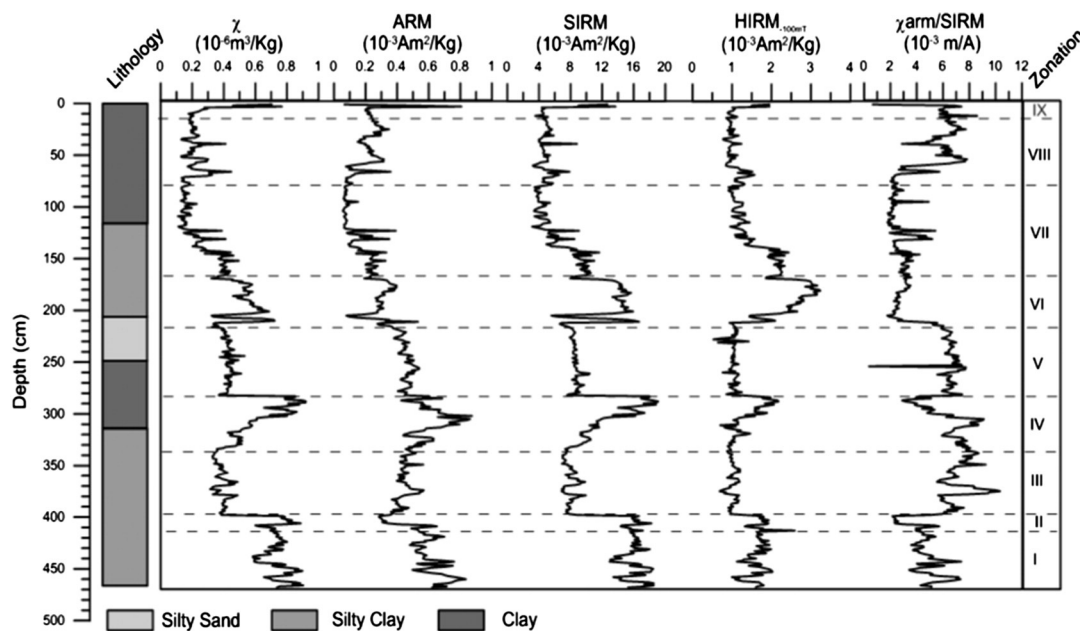


**Fig. 5.** Magnetic susceptibility ( $\chi$ ), anhysteretic remanent magnetization (ARM), saturation isothermal magnetization (SIRM), anhysteretic remanent magnetization–saturation isothermal magnetization ratio for the complete sequence. Zones I–IX are the result from the combined interpretation of  $\chi$ , ARM, SIRM and  $\chi_{\text{arm}}/\text{SIRM}$ , organic content, grain size and water content analyses.

surface of the floodplain, displayed two probable modern ages (Table 1) after calibration using the Bomb curve (Vogel et al., 2002), which indicates that the shells from the floodplain are relatively unaffected by the old-carbon sources available upstream. The age offset between the time of collection and calibrated age is maximum c. 50 years, which is small when considering the overall accuracy of the age model. The reason for the modern age of these shells is probably that these organisms are mainly using carbon from respired CO<sub>2</sub> derived from the plant remains that they consume, which is incorporated into the carbonate shells (Keith et al., 1962; McConaughey and Gillikin, 2008). Dissolved bicarbonate from humus acids is another source of terrestrial-derived carbon that these shells may use for their carbonate production (Keith et al., 1962). We assume that shells living in the Limpopo River floodplain are in balance with the atmospheric radiocarbon reservoir, which is further supported by the preferred environment of the fossil species dated. The freshwater gastropod shell, *Melanoides tuberculata* Müller, is known to thrive in calm waters with silty and muddy

sediments (Duggan, 2002), while the bivalve, *Corbicula fulminea* Müller, is usually found in fine-grained substrate and slow-moving waters (Schmidlin and Baur, 2007). The fact that the gastropods were found in an assemblage, and the bivalve with both valves attached, also suggests that they lived at or near the site at the time of burial, and that they were not transported before being deposited.

The interpretation of the date obtained from the wood fragment needs some consideration. The <sup>14</sup>C age of wood can be older than the maximum age of the tree from which it was derived because inner parts of a tree trunk and large branches may stop growing a significant number of years before the tree dies. In addition, it cannot be ruled out that the wood macrofossil was a product of re-deposition of secondary sediments with its origin upstream. Although these issues should be kept in mind, the coherent stratigraphical-chronological order of the wood fragment in relation to the other macrofossils, suggests that the wood combined with shells are the best option for an age-depth model construction.

**Table 2**

Summary of results for  $\chi$ , ARM, SIRM and  $\chi_{\text{arm}}/\text{SIRM}$ , organic content, grain size and water content analyses.

Zone	Depth (cm)	Zone description
IX	0–10	Increasing trends of $\chi$ (from $0.2 \times 10^{-6}$ to $0.4 \times 10^{-6} \text{ m}^3/\text{kg}$ ), ARM ( $0.1 \times 10^{-3}$ to $0.4 \times 10^{-3} \text{ Am}^2/\text{kg}$ ) and organic carbon content (1.4 to 1.7%). Considerable concentration of stable single domain particles displayed by the low values of $\chi_{\text{ARM}}/\text{SIRM}$ ( $0.6 \times 10^{-3} \text{ A/m}$ ).
VIII	10–72	Stable, with a minor peaks in $\chi$ ( $0.3 \times 10^{-6} \text{ m}^3/\text{kg}$ ), SIRM ( $0.3 \times 10^{-2} \text{ Am}^2/\text{kg}$ ) grain size (2%), and the ratio SIRM/ $\chi$ shows an increase and the average values $25.10^3 \text{ A/m}$ .
VII	72–167	A decreasing trend upwards for $\chi$ (from $0.4 \times 10^{-6}$ to $0.2 \times 10^{-6} \text{ m}^3/\text{kg}$ ) and SIRM ( $0.7 \times 10^{-2} \text{ Am}^2/\text{kg}$ ). The ratio SIRM/ $\chi$ shows an increase with a average of $25 \times 10^3 \text{ A/m}$ .
VI	167–215	Smooth decreasing trend upwards for $\chi$ with an average concentration of $0.5 \times 10^{-6} \text{ m}^3/\text{kg}$ and SIRM with an average concentration of $15 \times 10^{-4} \text{ Am}^2/\text{kg}$ . Decrease of water (12% dwt) and organic carbon (0.15%) contents. Peak in sand content (12%) followed by HIRM <sub>100</sub> , HIRM <sub>300</sub> and medium IRM. Larger ferrimagnetic particles dominate the sediment (low $\chi_{\text{ARM}}/\text{SIRM}$ ).
V	215–280	Low $\chi$ ( $0.4 \times 10^{-6} \text{ m}^3/\text{kg}$ ), SIRM ( $0.2 \times 10^{-3} \text{ Am}^2/\text{kg}$ ) and sand content (close to 0%). ARM shows a slightly decreasing trend upwards. $\chi_{\text{ARM}}/\text{SIRM}$ ( $0.7 \times 10^{-3} \text{ A/m}$ ) shows high values compared to zone IV, indicating dominance of stable-single domain particles.
IV	280–332	The $\chi$ values display a peak, with an average value of $0.7 \times 10^{-6} \text{ m}^3/\text{kg}$ . This peak is followed by peaks in ARM ( $0.6 \times 10^{-3} \text{ Am}^2/\text{kg}$ ), SIRM ( $14 \times 10^{-3} \text{ Am}^2/\text{kg}$ ), sand content (28%). The ratios $\chi_{\text{ARM}}/\text{SIRM}$ , HIRM <sub>100</sub> and medium IRM do follow the $\chi$ peak. The sediment is dominated by larger ferrimagnetic grain size (relatively high $\chi_{\text{ARM}}/\text{SIRM}$ ).
III	332–395	Low values of $\chi$ ( $0.4 \times 10^{-6} \text{ m}^3/\text{kg}$ ), SIRM ( $7 \times 10^{-3} \text{ Am}^2/\text{kg}$ ) and sand content (<1%).
II	395–410	Pronounced peaks in $\chi$ ( $0.8 \times 10^{-6} \text{ m}^3/\text{kg}$ ), SIRM ( $14 \times 10^{-3} \text{ Am}^2/\text{kg}$ ), sand content (20%), HIRM <sub>100</sub> and HIRM <sub>300</sub> . These coincide with low values of ARM ( $0.2 \times 10^{-2} \text{ Am}^2/\text{kg}$ ), $\chi_{\text{ARM}}/\text{SIRM}$ (close to 0) and organic carbon (0.5%). Larger magnetic grains (low $\chi_{\text{ARM}}/\text{SIRM}$ ) dominate the sediment.
I	410–468	Stable values with minor fluctuations in $\chi$ , ARM, SIRM, $\chi_{\text{ARM}}/\text{SIRM}$ , HIRM <sub>100</sub> and HIRM <sub>300</sub> .

#### 4.2. Lithology, sand content, organic carbon and water content

The abrupt peaks in sand content (Fig. 3) are probably a result of major flooding of the Limpopo River, resulting in inflow of large sediment particles that were allowed to settle when the flood withdrew. Apart from these clear sand peaks, neither the grain size analysis nor the visual inspection of the sediments suggest any additional disturbances in the sequence, but reveal a relatively homogenous composition throughout the core with only gradual shifts in lithology. The highest organic carbon values displayed in the lower section are probably the result of better conditions for preservation, i.e. higher moisture availability. Higher water levels are also suggested by the diatom assemblage in this part of the sequence, which we discuss below.

#### 4.3. Diatoms

A general feature of the studied sequence is the low occurrence of diatoms (Fig. 4a and b). In many cases the valves have been physically degraded, probably because of erosive processes during sedimentation and/or transportation, and perhaps due to the high pH and the presence of calcareous bedrocks, which may collectively degrade siliceous microfossils. Bearing these weaknesses in mind, three bio-stratigraphic zones were identified based on the diatom assemblage.

##### 4.3.1. Diatom zone 1 (468–280 cm, c. AD 1200–1400): Oxbow lake stage

Wet conditions prevailed at the site, either as open lake conditions or from riverine influences of the Limpopo River. The freshwater diatoms are dominated by *A. granulata*, which is a generalistic species that can live both in turbid rivers (O'Farrell et al., 2001; Risberg et al., 1999) and in lakes, tolerating fluctuations in water depth, conductivity and nutrient concentration (Izaguirre and Vinacur, 1994). Additional evidence of the freshwater influence is the presence of the gastropod *Melanoides tuberculata* (Müller, 1774), which prefer shallow lakes and tolerate a wide range of salinity (Dundee and Paine, 1977). Although *A. granulata* may tolerate turbid waters, the other taxa do not, suggesting that the site most likely experienced calm, lacustrine conditions during this period. The group of brackish-marine taxa includes species that tolerate a wide range of salinity concentrations; ranging from marine waters to inland waters with high electrolytic concentrations generated e.g. from highly evaporative conditions. Some taxa are strictly marine, such as *T. americana*, a species observed in coastal tropical and subtropical areas, including east Africa (Alhonen et al., 1984). Other strictly marine taxa identified in the present record are *Actinopychus* spp., *Coscinodiscus* sp. and *N. cocconeiformis* (cf. Asha Devi et al., 2010; Resende et al., 2007; Round and Basson, 1997; Sato et al., 2001). The presence of brackish-marine diatoms in general and strictly marine taxa in particular, suggests that the site was occasionally inundated by the sea during this period, probably during high tides. The presence of aerophilous taxa indicate that although the basin was water-filled, relatively dry conditions prevailed around the site. The aerophilous diatoms may originate from the littoral zone, perhaps a result of seasonal desiccation of the flood-plain area. Soil erosion upstream and transport of terrestrial material may have contributed to deposition of river bank sediments in our sampling site during flooding events.

##### 4.3.2. Diatom zone 2 (280–215 cm; c. AD 1400–1700): Transition zone

The diatom concentration decreases considerably, either due to worse conditions for preservation and/or due to the absence of favorable conditions for diatom growth. Both these factors are generally associated with lower water availability, which suggests drier conditions at the site compared to the underlying zone. The presence of the halophilous *C. meneghiniana*, however, indicates that there was still standing water, although with higher salinity than before, perhaps due to enhanced evaporation. The zone probably represents a transitional period where the oxbow lake became shallower due to sediment accumulation and a lower water level.

##### 4.3.3. Diatom zone 3 (215–0 cm; AD 1700–2000): Infilled lake

Decreasing diatom abundance and a dominance of aerophilous taxa (*H. amphioxys*, *N. goeppertiana*) suggest increased dryness compared to the previous zone with an environment free of standing water. This period, therefore, represents a basin filled with sediment, more or less covered with vegetation. One exception is present at 105 cm, where the freshwater planktonic taxon *Aulacoseira ambigua* occasionally appears in low numbers. Several diatom valves connected as original chains. This well-preserved state of the diatom valves indicates that *A. ambigua* was growing at the actual sampling site or transported only a short distance under calm conditions. As planktonic diatoms require substantial water depth for growth, this occurrence probably represent a short-lived lake environment centered at c. AD 1750 ± 50.

#### 4.4. Mineral magnetic parameters

The principle rationale behind mineral magnetic properties in paleoenvironmental studies is that the magnetic and morphological characteristics of the mineral grains can give information about shifts and variability in sediment provenance and transport processes. Magnetic susceptibility ( $\chi$ ) can indicate to what extent a material can be magnetized. This parameter is dependent on the concentration as well as the shape, size and mineralogy of the magnetic fraction in the sediment. In this record, variations in magnetic susceptibility are interpreted to be the results of changes in grain size (Šroubek et al., 2007) and not pedogenic processes (cf. Ellwood et al., 1996). The saturation isothermal remanent magnetization (SIRM) is a measure of the concentration of ferrimagnetic minerals, mainly magnetite (Thompson and Oldfield, 1986). Therefore, SIRM is affected by the source of the deposited sediments, i.e. the original bedrock from which sediments were formed. The Limpopo River carries eroded material from the upper drainage area in northern South Africa, where the dominant bedrock varies between gneiss, quartzite, metapelitic, amphibolite, marble, granite and charnockite (Brandl, 2001) and basalts from the Letaba-Pafuri group belonging the upper of the Karoo Super-group and limestone (GTK Consortium, 2006). Amphibolites are metamorphic rocks with a chemical composition comparable to basalts, and they include mainly plagioclase feldspar and hornblende, with minor inclusions of e.g. biotite, epidote, ganet, silimanite, titanite, ilmenite and magnetite (Chados and Engel, 1961). In addition, basalts contain a relatively high proportion of dense magnetite (Timberlake, 1998). Thus, sediments deposited at our site during high energy flooding events probably contain magnetite grains within in their load, which would cause enhanced SIRM-values. Between these events, the deposited sediments are transported by small local rivers, or from local sheet erosion, carrying mainly sediments originating from the local sand dunes, with low magnetic content.

The peaks in  $\chi$  and SIRM (Fig. 5), coincide with peaks in sand content (Fig. 3), particularly in zones II, IV and VI. These peaks are interpreted as the result of high energy fluvial transport, which would selectively bring coarse-grained detrital minerogenic-rich sediment to the sampling site from upstream sources (cf. Wolfe et al., 2006). This scenario is supported by low  $\chi_{ARM}$ /SIRM and organic carbon values as a result of the dominance of relatively large multi-domain particles and an input of clastic minerogenic particles in general. The peaks in  $\chi$  and SIRM are generally characterized by abruptness, particularly in the termination of the events. These abrupt transitions are interpreted to be erosive, probably caused by occasional re-opening of the oxbow lake by the Limpopo River. Termination of the flooding event is characterized by gradual decline in mineral magnetic proxies (e.g. at the transition between zone VI and VII) and interpreted as soil-formation stage. These differences probably reflect the type of environment in which they are recorded; a lake (lower half of the record), versus a terrestrial environment with active soil formation processes (upper half of the record). Since the flooding event at the VI/VII-boundary the river never re-opened the relic oxbow lake and the varying sediment accumulation therefore would depend on differences in flooding intensities and durations of terrestrial

conditions only. The amplitude of the strong signals seen in the various parameters in zones II, IV and VI suggest that these peaks represent periods of high magnitude flooding events. One (or several) of the modern, last-century flooding events might be recorded in zone IX, reflected that has relative high concentrations of  $\chi$ , ARM and SIRM in the uppermost zone.

Bi-plots of the mineral magnetic properties can be used to more clearly illustrate the relation between proxy-data and the suggested relation to flooding events (Fig. 6a). The bi-plot of SIRM vs  $\chi$  (Fig. 6a) illustrates that samples interpreted as signals of flooding events (zones II, IV and VI) have high values of  $\chi$  and SIRM, as do samples from the oxbow lake (zone I). This distribution is caused by in-wash of ferrimagnetic magnetite grains of stable single domain character, e.g. magnetite, during flooding events. The bi-plot SIRM vs. ARM (Fig. 6b) similarly shows that samples representative of flooding events display high SIRM and ARM-values, as do samples from the oxbow lake stage (zone I). Samples from soil formation stages show low values of both ARM and SIRM. This distribution indicates that the site was affected by inwash of eroded soil during flooding events. These events were probably more frequent during the lake stages, which is generally characterized by a higher concentration of magnetic minerals in the lowermost sequence. Several minor

floods probably affected the site during this stage, strong enough to leave minerals with low magnetic signatures, but not strong enough to imprint peak-events in our proxies.

From the bi-plot showing sand content vs.  $\chi$  (Fig. 6c) we suggest threshold values for both parameters, above which high magnitude flooding events are likely recorded at the site. Peaks in both parameters are suggested to represent flooding events and sand contents are higher than 5% and  $\chi$  is greater than  $0.4 \times 10^{-6} \text{ m}^3 \text{ kg}^{-1}$ . Each level with higher concentrations of sand content is here suggested to represent a flooding event. The record reveal three occasions with flooding of this magnitude at the site, probably associated with intense and/or more frequent rainfall within the drainage area of the Limpopo River; at c. AD 1260 ± 60, 1385 ± 75 and 1565 ± 75.

## 5. Discussion

### 5.1. Local development of the site: Influences of flooding and sea level change

The Indian Ocean tidal range at the mouth of Limpopo River is on the order of ± 4–5 m. Thus, at present, our sampling site is situated at 6 m a.s.l., and is not exposed to a direct marine influence. Around AD 1200,

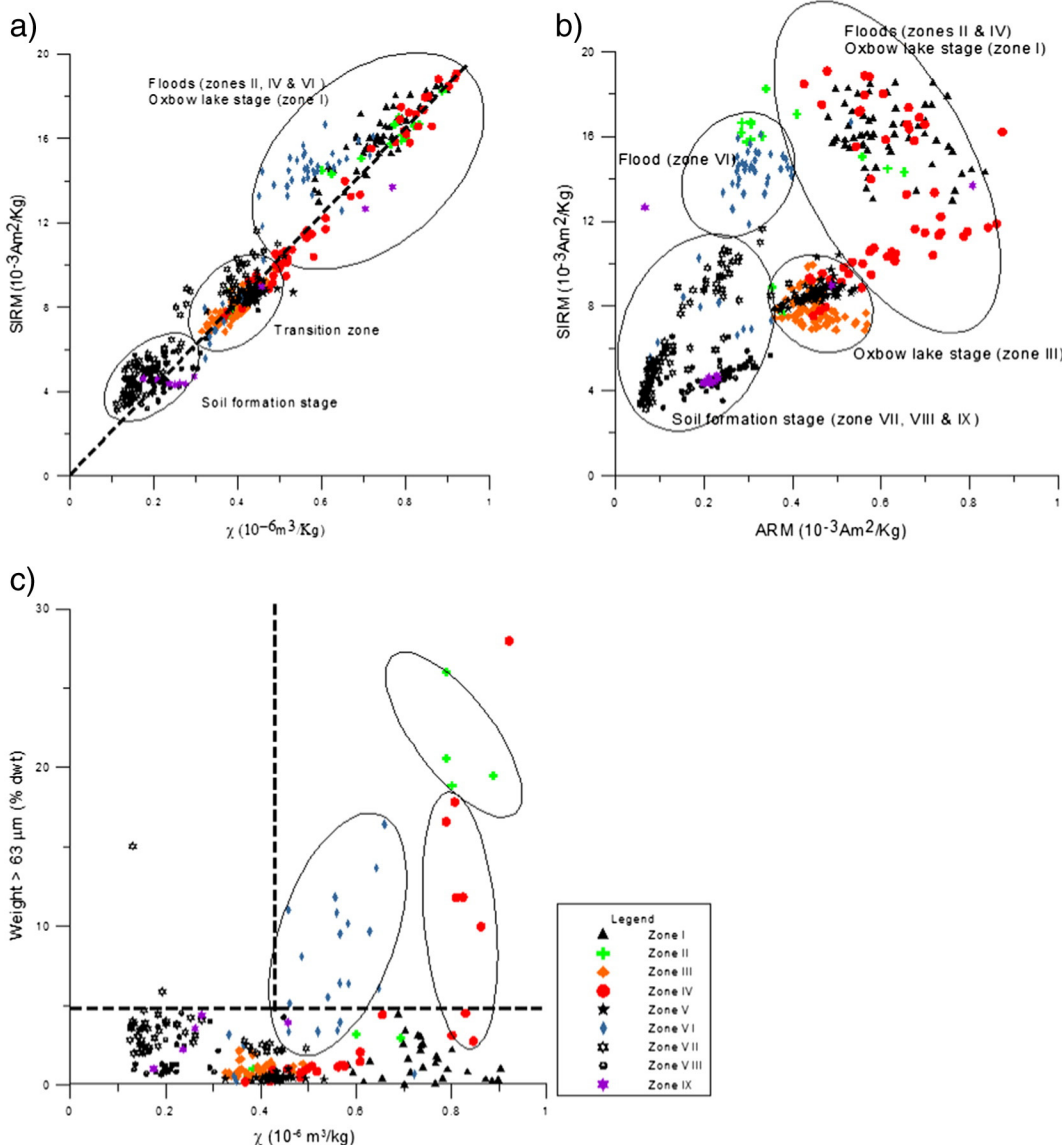


**Fig. 6.** Selected mineral magnetic parameters ( $\chi$ , SIRM and ARM) and sand content plotted against each other. Note that each ellipse contains the majority of samples representing the stated zones, but may also contain a number of samples from other zones. The dashed lines in panel c represent threshold values to define sediment characteristics for the flooding events.

however, the flood plain surrounding the sampling site was at a lower altitude in relation to sea level. Since the onset of our record, c. 4.5 m of sediment has been accumulated (in the floodplain), indicating a lower topographic position in relation to the contemporary sea level at that time compared to today. Furthermore, considering that sea level changed in the past, including the late Holocene (e.g. Compton, 2006; Norström et al., 2012; Ramsay and Cooper, 2002), it is likely that the site previously was affected by influx of sea waters. A coastal paleo-environmental study from southern Mozambique suggests that sea levels were higher than present c. 1000 years ago (Norström et al., 2012). This is also inferred by other local (Ramsay and Cooper, 2002) and regional-scale (Compton, 2006) sea-level records from southern Africa, suggesting a relative lowering of sea level in the order of 1.5 and 0.5 m respectively. Thus, it is likely that tidal inundation from the Indian Ocean brought marine diatoms to our site between c. AD 1200 and 1400, when both marine and brackish-marine diatoms appear in the assemblage. The interpretation is supported by the absence of diatoms able to withstand variations in osmotic pressure which makes it unlikely that increase in marine-brackish taxa is a result of increased evaporation rates (cf. Izaguire and Vinacur, 1994). Keeping the limitations of the age model in mind, it can be noted that the sedimentation rate at our site was on average c. 8 mm/year during this lake-stage, most likely dominated by shore in-wash and organic production within the lake. As time progressed, repeated flooding events contributed to the sediment deposition in the oxbow lake, which finally transformed into a vegetated, terrestrial environment.

The distinct peaks in sand content and mineral magnetic concentration (SIRM and  $\chi$ ) suggest that the oxbow lake was affected by river-water fluxes, which can be related to high-energy water flow during the initial stage of a flooding event (Wolfe et al., 2006). Four such events are detectable in our record; in the mid-1200 AD, late-1300 AD, mid-1500 AD and during the last century. The visual sediment lithology indicates gradational boundaries between lithological units; hence, no indications of erosive hiatuses can be identified from the visible inspection of the lithology. However, the generally abrupt termination of the peaks in the flooding-proxies (i.e. grain-size and mineral magnetic properties) is a sign of erosion and the presence of hiatuses in our record. Erosional processes are likely to be more effective as the oxbow lake becomes filled with sediments, with the result that the record becomes less complete as time progresses. Thus, the open lake environment is probably better suited for picking up signals of flooding events, as it represents a protected basin filled with water, where river-sediments from the flood are allowed to stay and settle, and where erosive processes are of minor importance.

Evidence of the major flooding event in AD 2000 is difficult to identify from the present sequence due to age-depth model constraints, however, the peak in mineral magnetic parameters in zone IX (Fig. 4) may represent this event and/or one of the other flooding events that affected the area during the last century (Direcção Nacional de Águas, 1996; INGC et al., 2003). The fact that only one “modern” flooding event is recorded in our dataset, demonstrates that the magnitudes of older paleoflooding events observed in the record were probably higher than the average magnitude of the historically documented 20th century flooding events. Additionally, erosion during flooding may have removed sediments due to the flat topography of the recent site, as discussed above.

Of course, there is a limit of how representative one site is for the entire flood-plain. The Limpopo River flood-plain occupies a wide geographical area and has a number of sedimentary sub-environments. The character of the stratigraphic evidences from each flooding event would vary from one place to another. The four high-magnitude flooding events observed in our study are a minimum for the Limpopo flood-plain area and further studies are likely to reveal additional events.

## 5.2. Regional comparison and connections to regional climate

The observed paleo-environmental changes and paleo-flooding in our sediment sequence are mainly determined by variations in hydro-

climate, i.e. evaporative effects as well as precipitation changes within the drainage area. Other paleo-environmental records from the region show variations in hydrological conditions during the last millennium (e.g. Ekblom and Stabell, 2008; Ekblom et al., 2012; Holmgren et al., 2003, 2012; Neumann et al., 2010; Stager et al., 2013). The paleoclimatic records from Makapansgat Valley in South Africa (Holmgren et al., 2003), and from the lower Limpopo Valley (Ekblom et al., 2012) are significant for our study as they are located within the Limpopo River drainage area (Fig. 1). Although dating uncertainties hamper a detailed comparison between records, the two earliest indications of floods in our sequence (mid-1200 and late-1300 AD) probably occurred when regional climate situation was generally wet and warm. The Makapansgat isotopes registered generally warmer and wetter conditions (Holmgren et al., 2003) from 1200 to 1500 AD, and the lower Limpopo Valley experienced wetter conditions between 800 and 1400 AD (Ekblom et al., 2012). Between 1100 and 1400 AD diatom analysis on lake sediments from Lake Nhaucati, southern Mozambique (Ekblom and Stabell, 2008), also indicate high lake-levels and wetter conditions when our two earliest reconstructed flooding event occurred (mid-1200 AD and late-1300 AD). Diatom analysis of sediment in Lake Sibaya at the South African coast (Stager et al., 2013) and Lake Nhauhache, southern Mozambique (Holmgren et al., 2012) however suggest that generally dry conditions prevailed from c. AD 1200 until AD 1700, although the period AD 1470 to AD 1540 was wet at Lake Sibaya (Stager et al., 2013).

The third period of flooding inferred from our Limpopo flood-plain site (c. mid-1500 AD) coincides with a transition from warm/wet to cold/dry conditions according to Makapansgat data (Holmgren and Öberg, 2006; Holmgren et al., 2001; Lee-Thorp et al., 2001). Lower Limpopo Valley records also suggest dry conditions during this period (Ekblom et al., 2012), and so does Lake Nhauhache, southern Mozambique (Holmgren et al., 2012). In general, indications of dryness have been recorded in proxy data obtained from several sites in the region at his time, particularly after c. 1500 AD (Ekblom and Stabell, 2008; Ekblom et al., 2012; Holmgren et al., 2003, 2012; Neumann et al., 2010; Norström et al., 2005, 2008; Smith et al., 2007; Stager et al., 2013). The indications of a drier climate coincide with signals that the oxbow lake became filled with sediment. Possibly, increased regional dryness contributed to lowering of the lake level at our site, which accelerated sedimentation rates and *in situ* accumulation due to decreased vegetation cover.

In summary, the flooding events that our proxy record identifies at mid-1200 AD and late 1300 AD can probably be correlated to periods of enhanced regional precipitation, as they took place during regionally wet and warm climate conditions. Wet conditions are generally associated with a higher risk of flooding, due to higher annual rainfall amounts in combination with saturated soils that have lower infiltration capacity. However, the mid-1500 AD flooding event identified in our record took place during overall cold-dry period. In southern Africa, the riverine environments during dry periods are sensitive to extreme rainfall events, e.g. due to large exposed areas and sparser vegetation cover. The vegetation acts in a protective manner, both in the role as a water consumer and soil binder, which limit the effectiveness of erosional processes and mitigate the effects of flooding. Thus, during prolonged dry periods, flooding is probably more likely to affect the landscape by through erosion which results in stronger imprint on sedimentary sequences.

## 5.3. Evaluation of methods for paleo-flood reconstruction

We present a methodology for studying oxbow lake sediments as proxies for paleo-flooding and paleo-environmental reconstruction in the Limpopo floodplain, and argue that despite their very complex formation they can be used for studying flooding events. Among the studied parameters, we found that sediment grain size and mineral magnetic properties of the minerogenic fraction have the ability to

detect signals from high-intensity river-discharge events. More specifically, the sand content, as well as the mineral magnetic parameters, seem to be the most sensitive proxies in terms of reconstructing flooding of the Limpopo River plain. This methodology may be used also in other regions, particularly the grain size approach, while the magnetic parameters can be more local in their suitability for identifying flooding events because of geological factors that require differences in provenance and/or signals caused by sediment sorting processes.

Diatoms are widely used as proxies of diverse environmental and climate changes, due to their ability to respond to physical and chemical forcing factors in various parts of the world. In southern Africa they have been applied to reconstruct wet and dry periods from lake sediments (Ekblom and Stabell, 2008; Gasse et al., 1997; Holmgren et al., 2012) and to trace sea-level changes (Norström et al., 2012). In this study, the fossil diatoms assemblage was used to reconstruct the gradual development of the studied oxbow lake and the associated environments. However, the low abundance of diatoms limited the use of this method, particularly in terms of identifying short-term events such as flooding.

Dating of river-related sediments is a difficult task and from this study we can conclude that the best option, at least in this region, is to use shell material for <sup>14</sup>C-dating rather than from bulk sediment. The reasons are that 1) modern ages of the living shells in the flood plain suggest that they produce their shells in balance with the atmospheric radiocarbon reservoir, and 2) the preferred habitat of the fossil shells relates to the floodplain environment rather than the upstream reworked sediments, which is also supported by the fact that the fossils were found in a well preserved state.

## 6. Conclusions

This paper reports the first stratigraphic analyses of sediments from the vast Limpopo River flood-plain, Mozambique. The major conclusions are as follows:

- Analysis of mineral magnetic parameters and grain-size variations allowed the identification of past flooding events at the site. Magnetic susceptibility, saturation isothermal magnetization (SIRM) and sand content were the most sensitive proxies in terms of reflecting paleo-flooding.
- Four high-magnitude flooding events were identified during the last c. 800 years in the flood plain; in mid-1200s, late-1300s, mid-1500s and during the last century.
- Diatom analyses indicate that the sampling site acted as a lake between c. AD 1200 and AD 1400. During this period, the site was occasionally inundated by marine waters, perhaps due to higher sea-levels during late Holocene. After c. AD 1400 the basin became drier and was completely dried up at mid-1500 AD, when it became a ground surface that was covered with water only during flooding events.
- The individual flooding events identified in our record are not entirely correlated to periods of enhanced regional precipitation, but seems to appear both during regionally wet and dry climate conditions. This stresses the importance of 1) additional and extended paleo-flooding reconstructions that may eventually contribute to qualitative forecasting of such events and 2) the need of better knowledge on regional rainfall variability, particularly the spatial distribution, frequency and intensity of extreme rainfall events, and their impact as triggers of flooding events.

The outcome of the mineral magnetic and grain size analysis is promising for a future extension of this study to cover several cores in the flood-plain, which would allow for a more complete reconstruction of the region's flooding history. Such information is central for improved predictions and for societal management associated with mitigation of future flooding events that may affect the Limpopo floodplain.

## Acknowledgments

The research was funded by the SIDA/SAREC (Swedish International Development Cooperation Agency/Swedish Agency for Research Cooperation) and VR (the Swedish Research Council). Dr. Eve Arnold and Åsa Wallin, Department of Geological Sciences, Stockholm University, assisted during grain size analyses. Elidio Massuanganue from Department of Geology, Eduardo Mondlane University, participated in the field work. Dr. Dai G. Herbert, the Natal Museum, helped with shell identification. Hildred Crill, Dr. Anneli Ekblom and an anonymous reviewer gave valuable input on the manuscript.

## References

- Alhonen, P., Heino, A., Tynni, R., 1984. Über vorkommen und bedeutung von *Terpsinoë americana* (Bail.) Ralfs in den Ablagerungen des Litorinameeres. Bull. Geol. Soc. Finl. 56 (1–2), 117–133.
- Asha Devi, C.R., Jyothibabu, R., Sbu, P., Jacob, J., Habeebrehman, H., Prabhakaran, M.P., Jayalakshmi, K.J., Achuthankutty, C.T., 2010. Seasonal variations and trophic ecology of microzooplankton in the southeastern Arabian Sea. Cont. Shelf Res. 30, 1070–1084.
- Battarbee, R.W., 1986. Diatom analysis. In: Berglund, B.E. (Ed.), Handbook of Holocene Palaeoecology and Paleo hydrology. John Wiley & Sons Ltd., Chichester, pp. 527–570.
- Brandl, G., 2001. Explanation: Geological map of the Limpopo Belt and its environs (1:500 000). Council for Geoscience, Pretoria, South Africa, 46 pp.
- Cardoso, A.F., 2009. Registro Instrumental das Inundações na Região Sul de Moçambique e sua relação com o clima. Projeto Científico, Departamento de Geologia, Universidade Eduardo Mondlane, Maputo, Moçambique.
- Chadost, A.A., Engel, C.G., 1961. Fluorescent X-ray spectrographic analyses of amphibolite rocks. Am. Mineral. 46, 120–133.
- Cholnoky, B.J., 1957. Beiträge zur Kenntnis der Südafrikanischen Diatomeenflora. Port. Acta Biol. (B) VI, 53–93.
- Compton, J.S., 2006. The mid-Holocene sea-level highstand at Bogenfels Pan on the southwest coast of Namibia. Quatern. Res. 66, 303–310.
- Direcção Nacional de Águas (DNA), 1996. Monografia Hidrográfica da Bacia do Rio Limpopo (Eng: Hydrological Monograph on the Limpopo River Basin). Report no. 16/96, pp. 28–102 (Maputo).
- Duggan, I.C., 2002. First record of a wild population of the tropical snail *Melanoides tuberculata* in New Zealand natural waters. N. Z. J. Mar. Freshwat. Res. 36, 825–829.
- Dundee, D.S., Paine, A., 1977. Ecology of the snail, *Melanoides tuberculata* (Müller), intermediate host of the human liver fluke (*Opisthorchissinensis*) in New Orleans, Louisiana. Naultinus 91, 17–20.
- Dyson, L.L., Von Heerden, J., 2001. The heavy rainfall and floods over the northeastern interior of South Africa during February 2000. S. Afr. J. Sci. 97, 80–86.
- Ekblom, A., Stabell, B., 2008. Paleohydrology of Lake Nhauacuti (southern Mozambique) ~400 AD to present. J. Paleolimnol. 40, 1127–1141.
- Ekblom, A., Gillson, L., Risberg, J., Holmgren, K., Chidou, Z., 2012. Rainfall variability and vegetation dynamics of the lower Limpopo Valley, Southern Africa, 500 Ad to present. Palaeogeogr. Palaeoclimatol. Palaeoecol. 363, 69–78.
- Ellwood, B.B., Petruso, K.M., Horrold, F.B., Korkuti, M., 1996. Paleoclimate characterization and intra-site correlation using magnetic susceptibility measurements: an example from Konispol Cave, Albania. J. Field Archaeol. 23, 263–271.
- Foged, N., 1975. Some littoral diatoms from the coast of Tanzania. Bibliotheca Phycologica Band 16. J. Cramer, Vaduz, p. 126.
- Gasse, F., 1986. East African diatoms: taxonomy, ecological distribution. Bibliotheca Diatomologica Band 11. J. Cramer, Berlin, p. 201.
- Gasse, F., Barker, P., Fritz, S.C., Chaile, F., 1997. Diatom-inferred salinity in paleolakes: an indirect tracer of climate change. Quat. Sci. Rev. 16, 547–563.
- Giffen, M.H., 1963. Contributions to the diatom flora of South Africa: I. Diatoms of the Estuaries of the Eastern Cape Province. Hydrobiologia XXI, 200–265.
- Giffen, M.H., 1966a. Contributions to the diatom flora of Southern Africa II. Nova Hedwigia 21, 122–150.
- Giffen, M.H., 1966b. Contributions to the diatom flora of South Africa. Nova Hedwigia XIII, 245–291.
- Giffen, M.H., 1970. New and interesting marine and littoral diatoms from Sea Point, near Cape Town, South Africa. Bot. Mar. XIII, 87–99.
- Giffen, M.H., 1971. Marine diatoms from the Gordon's Bay, Region of False Bay, Cape Province, South Africa. Bot. Mar. XIV, 1–16.
- Giffen, M.H., 1973. Diatoms of the marine littoral of Steenberg's Cove in St. Helena Bay, Cape Province, South Africa. Bot. Mar. XVI, 32–48.
- Giffen, M.H., 1975. An account of the littoral diatoms from Langebaan, Saldanha Bay, Cape Province, South Africa. Bot. Mar. XVIII, 71–95.
- Giffen, M.H., 1976. A further account of the marine littoral diatoms of the Saldanha Bay Lagoon, Cape Province, South Africa. Bot. Mar. XIX, 379–894.
- GTK Consortium, 2006. Map Explanation: Volume 1: Sheets 2032–2632. Geology of Degree Sheets, Espungabera/Chibabava, Nova/Mambone, Massangena, Chidoco, Save/Bazaruto, Chicualacuala, Machaíla, Chigubo, Mabote/Vilanculos, Rio Singuézzi/Massingir, Rio Changana, Funhalouro/Inhambaré, Chilembene, Chókwè, Zavala/Inharrime, Maputo, Xai-Xai/Zavala and Bela-Vista, Mozambique. Ministério dos Recursos Minerais, Direcção Nacional de Geologia, Maputo, pp. 220–234.
- Hattingh, J., Zawada, P.K., 1996. Relief peels in the study of paleoflood slack-water sediments. Geomorphology 16, 121–126.
- Hegerl, G.C., Russion, T., 2011. Using the past to predict the future? Science 334, 1360–1361.

- Heine, K., Heine, J.T., 2002. A paleohydrological reinterpretation of the Homeb silts, Kuiseb River, central Namib Desert (Namib) and paleoclimatic implications. *Catena* 48, 107–130.
- Holmgren, K., Öberg, H., 2006. Climate change in southern and eastern Africa during the past millennium and its implications for societal development. *Environ. Dev. Sustain.* 8, 185–195.
- Holmgren, K., Moberg, A., Svanered, O., Tyson, P.D., 2001. A preliminary 3000-year regional temperature reconstruction for South Africa. *S. Afr. J. Sci.* 97, 49–51.
- Holmgren, K., Lee-Thorp, J.A., Cooper, G.R.J., Lundblad, K., Partridge, T.C., Scott, L., Sthaldeen, R., Talma, A.S., Tyson, P.D., 2003. Persistent millennial-scale climatic variability over the past 25000 years in southern Africa. *Quat. Sci. Rev.* 22, 2311–2326.
- Holmgren, K., Risberg, J., Freudendahl, J., Achimo, M., Ekblom, A., Norström, E., Mugabe, J., Sitoé, S., 2012. Lake level variations at Lake Nhauhache, Mozambique, during the last 2300 years. *J. Paleolimnol.* 48 (2), 311–322.
- INGC (Instituto Nacional de Gestão de Calamidades), Universidade Eduardo Mondlane (UEM), FEWS NET, 2003. Atlas for disaster preparedness and response in the Limpopo Basin, (Maputo: 99 pp.).
- IPCC, 2013. Summary for Policymakers. In: Stocker, T.F., Qin, D., Plattner, G.-K., Tignor, M., Allen, S.K., Boschung, J., Nauels, A., Xia, Y., Bex, V., Midgley, P.M. (Eds.), Climate Change 2013: The Physical Science Basis Contribution of Working Group I to the Fifth Assessment Report of the Intergovernmental Panel on Climate Change. Cambridge University Press, Cambridge, United Kingdom and New York, NY, USA.
- Izaguirre, I., Vinacur, A., 1994. Algal assemblages from shallow lakes of the Salado River Basin (Argentina). *Hydrobiologia* 289, 57–64.
- Keith, M.L., Anderson, G.M., Eiceler, R., 1962. Carbon and oxygen isotopic composition of mollusk shells from marine and fresh-water environments. *Geochim. Cosmochim. Acta* 28, 1757–1786.
- Krammer, K., Lange-Bertalot, H., 1986. *Bacillariophyceae*. In: Ettl, H., Gerloff, J., Heyning, H., Mollenhauer, D. (Eds.), 1. Teil: *Naviculaceae*. *Süßwasserflora von Mitteleuropa* 2/1. Gustav Fischer Verlag, Stuttgart.
- Krammer, K., Lange-Bertalot, H., 1988. *Bacillariophyceae*. In: Ettl, H., Gerloff, J., Heyning, H., Mollenhauer, D. (Eds.), 2. Teil: *Bacillariaceae*, *Epithemiaceae*, *Surirellaceae*. *Süßwasserflora von Mitteleuropa* 2/2. Gustav Fischer Verlag, Stuttgart.
- Krammer, K., Lange-Bertalot, H., 1991a. *Bacillariophyceae*. In: Ettl, H., Gerloff, J., Heyning, H., Mollenhauer, D. (Eds.), Teil: *Centrales*, *Fragilariaeae*, *Eunotiaceae* *Süßwasserflora von Mitteleuropa* 2/3. Gustav Fischer Verlag, Stuttgart.
- Krammer, K., Lange-Bertalot, H., 1991b. *Bacillariophyceae*. In: Ettl, H., Gärtner, G., Gerloff, J., Heyning, H., Mollenhauer, D. (Eds.), 4. Teil: *Achnanthaceae*. Kritische Ergänzungen zu *Navicula* (Lineolate) und *Gomphonema*. *Süßwasserflora von Mitteleuropa* 2/4. Gustav Fischer Verlag, Stuttgart.
- Lee-Thorp, J.A., Holmgren, K., Lauritzen, S.E., Linge, H., Moberg, A., Partridge, T.C., Stevenson, C., Tyson, P., 2001. Rapid climate shifts in the southern African interior throughout the mid to late Holocene. *Geophys. Res. Lett.* 28, 4507–4510.
- McConaughey, T.A., Gillikin, D.P., 2008. Carbon isotopes in mollusk shell carbonates. *Geo-Mar. Lett.* 28, 287–299. <http://dx.doi.org/10.1007/s00367-008-0116-4>.
- McCormac, F.G., Hogg, A.G., Blackwell, P.G., Buck, C.E., Higham, T.F.G., Reimer, P.J., 2004. SHCal04 Southern Hemisphere calibration, 0–11.0 cal kyr BP. *Radiocarbon* 46 (3), 1087–1092.
- Mélice, J.C., Reason, C.J.C., 2007. Return period of extreme rainfall at George, South Africa. *S. Afr. J. Sci.* 103, 499–501.
- Neumann, F.H., Scott, L., Bousman, C.B., van As, L., 2010. A Holocene sequence of vegetation change at Lake Eteza, coastal KwaZulu-Natal, South Africa. *Rev. Palaeobot. Palynol.* 162, 39–53.
- Norström, E., Holmgren, K., Mört, M., 2005. Variations in d<sub>13C</sub>composition and wood anatomy in *Breonadia salicina* trees from South Africa between 1375–1995 AD. *S. Afr. J. Sci.* 101, 162–168.
- Norström, E., Holmgren, K., Mört, C.-M., 2008. A 600 year long d<sub>18O</sub>-record from cellulose of *Breonadia salicina* trees, South Africa. *Dendrochronologia* 26, 21–33.
- Norström, E., Risberg, J., Gröndahl, H., Holmgren, K., Snowball, I., Mugabe, J., Sitoé, S., 2012. Coastal paleo-environment and sea-level change at Macassa Bay, southern Mozambique, since c 6600 cal yrs BP. *Quat. Int.* 260, 153–163.
- O'Farrell, I., Tell, G., Podlejski, A., 2001. Morphological variability of *Aulacoseira granulata* (Ehr.) Simonsen (Bacillariophyceae) in the Lower Paraná River (Argentina). *Limnology* 2, 65–71.
- Ramsay, P.J., Cooper, J.A.G., 2002. Late Quaternary sea-level change in South Africa. *Quatern. Res.* 57, 82–90.
- Reason, C.J.C., 2007. Tropical cyclone Dera, the unusual 2000/01 tropical cyclone season in the southwest Indian Ocean and associated rainfall anomalies over southern Africa. *Meteorol. Atmos. Phys.* 97, 181–188.
- Reason, C.J.C., Keibel, A., 2004. Tropical cyclone Eline and its unusual penetration and impacts over the southern Africa Mainland. *Weather Forecast.* 19, 789–805.
- Resende, P., Azeiteiro, U.M., Gonçalves, F., Pereira, M.J., 2007. Distribution and ecological preferences of diatoms and dinoflagellates in the west Iberian coastal zone (north Portugal). *Acta Oecol.* 32, 224–235.
- Risberg, J., 1988. *Terpsinoë americana* (Bailey) Ralfs, a rare species in the Baltic fossil diatom flora. In: Round, F. (Ed.), Proceedings 9th Diatom-Symposium 1986, pp. 207–218.
- Risberg, J., Sandgren, P., Teller, J.T., Last, W.M., 1999. Siliceous microfossils and mineral magnetic characteristics in a sediment core from Lake Manitoba, Canada: a remnant of glacial Lake Agassiz. *Can. J. Earth Sci.* 36, 1299–1314.
- Round, F.E., Basson, P.W., 1997. A new diatom genus (*Giffenia*) based on *Nitzschia cocconeiformis* Grun. and a note on *Nitzschia (Tryblionella) lanceolata* Grun. *Diatom. Res.* 12, 347–355.
- Round, F.E., Crawford, R.M., Mann, D.G., 1990. The diatoms: biology & morphology of the genera. Cambridge University Press, Cambridge.
- Sato, H., Okuno, J., Nakada, M., Maeda, Y., 2001. Holocene uplift derived from relative sea-level records along the coast of western Kobe, Japan. *Quat. Sci. Rev.* 20, 1459–1474.
- Schmidlin, S., Baur, B., 2007. Distribution and substrate preference of the invasive clam *Corbicula fluminea* in the river Rhine in the region Basel (Switzerland, Germany, France). *Aquat. Sci.* 69, 153–161.
- Smith, A.M., 1991. Extreme paleofloods: their climatic significance and the chances of floods of similar magnitudes recurring. *S. Afr. J. Sci.* 87, 219–220.
- Smith, A.M., Zawada, P.K., 1990. Palaeoflood hydrology: a tool for South Africa? – An example from the Crocodile River near Brits, Transvaal, South Africa. *Water SA* 16, 195–200.
- Smith, J., Lee-Thorp, J., Hall, S., 2007. Climate change and agropastoralist settlement in the Shashe-Limpopo river basin, southern Africa: AD 880 to 1700. *S. Afr. Archaeol. Bull.* 62, 115–125.
- Šroubek, P., Diehl, J.F., Kadlec, J., 2007. Historical climatic record from flood sediments deposited in the interior of Spiralka Cave, Czech Republic. *Palaeogeogr. Palaeoclimatol. Palaeoecol.* 251, 547–562.
- Stager, J.C., Ryves, D.B., King, C., Madson, J., Hazzard, M., Neumann, F.H., Maud, R., 2013. Late Holocene variability in the summer rainfall region of South Africa. *Quat. Sci. Rev.* 67, 105–120.
- Stal, M., 2011. Flooding and relocation: the Zambezi River Valley in Mozambique. *Int. Migr.* 49, 125–145.
- Thompson, R., Oldfield, F., 1986. Environmental Magnetism. Allen and Unwin, London (227 pp.).
- Timberlake, J., 1998. Biodiversity of the Zambezi wetlands: review and preliminary assessment of available information, phase 1, February 1998. Consultancy Report for IUCN. The World Conservation Union, Regional Office for Southern Africa (IUCN ROSA), Harare, Zimbabwe.
- Vogel, J.C., Fulz, A., Visser, E., 2002. Accurate dating with radiocarbon from the atom bomb test. *S. Afr. J. Sci.* 98, 437–438.
- Vos, P.C., De Wolf, H., 1993. Diatoms as a tool for reconstructing sedimentary environments in coastal wetlands: methodological aspects. *Hydrobiologia* 269 (270), 285–296.
- Witkowski, A., Lange-Bertalot, H., Metzeltein, D., 2000. Diatom flora of Marine Coasts I. Koeltz Scientific Books, Königstein, p. 925.
- Wolfe, B.B., Hall, R.I., Last, W.M., Edwards, T.W.D., English, M.C., Karst-Riddoch, T.L., Paterson, A., Palmini, R., 2006. Reconstruction of multi-century flood histories from oxbow lake sediments, Peace-Athabasca, Canada. *Hydrol. Process.* 20, 4131–4153.